



# Electron Paramagnetic Resonance and Evaluation of Some Parameters of Mn-Doped BaMgAl<sub>10</sub>O<sub>17</sub> Phosphor

Vijay Singh <sup>1, \*</sup>; N. Singh <sup>1</sup>; G. Sivaramaiah <sup>2</sup>; A. S. Nagpure <sup>3</sup>;  
J. L. Rao <sup>4</sup>; S. Kokate <sup>5</sup> & Manoj K Tiwari <sup>6</sup>

<sup>1</sup>Department of Chemical Engineering, Konkuk University, Seoul, 05029, Republic of Korea

<sup>2</sup>Department of Physics, Government College for Men (Autonomous), Kadapa 516004, India

<sup>3</sup>Department of Applied Physics, MIET, Kudwa Village, Gondia, 441614, India

<sup>4</sup>Department of Physics, Sri Venkateswara University, Tirupati 517 502, India

<sup>5</sup>Department of Physics, SIRTS, Bhopal 462043, India

<sup>6</sup>Department of Physics, MIET, Shahapur, Bhandara 441906, India

vijayjiin2006@yahoo.com

## Abstract:

*In this work, we stabilize Mn in its 2+ state in the BaMgAl<sub>10</sub>O<sub>17</sub> (BAM) matrix using the combustion route without a further calcining treatment. X-ray diffraction (XRD) and energy dispersive spectroscopy (EDX) measurements were used to characterize the as-prepared combustion products. From the EPR data, the relaxation-time values were estimated for the system along with other EPR parameters.*

**Keywords:-** Ginger, Lemon, , Soft drink, Squash, Polyphenols.

## 1. Introduction

In recent years, Mn<sup>2+</sup>-activated phosphors have gained much attention due to its excellent electric, magnetic and optical properties [1-3]. BaMgAl<sub>10</sub>O<sub>17</sub> (BAM) is a well-known host matrix for doping of transition metals and rare earths ions [4-6]. To the best of the authors' knowledge, a dearth exists regarding the reports on EPR of Mn<sup>2+</sup>-doped BAM compared with other hosts, and particularly regarding the performance of a spectroscopic study in this host matrix, an extensive paper has not been published. It has been noted, that BAM has been traditionally prepared using solid-state reactions, which generally require long durations and high annealing temperatures [6]. In consideration of this, a successful preparation of the Mn<sup>3+</sup>-doped BAM phosphor via a simple and inexpensive solution-combustion process was completed for the present study to understand the role of the Mn<sup>2+</sup> in the BAM matrix.

## 2. Experimental

BaMgAl<sub>10</sub>O<sub>17</sub> doped with Mn<sup>2+</sup> ions was prepared by a solution combustion method. Barium nitrate, magnesium nitrate and aluminum nitrate were used in a typical synthesis as oxidizers, with carbonylhydrazide as fuel and MnCl<sub>2</sub>·4H<sub>2</sub>O as dopant precursors. The oxidizer: fuel ratio was calculated based on valencies of oxidizer (O) and fuel (F) of the reactants, keeping O/F = 1, as reported in an earlier paper. The starting materials were dissolved in a minimum quantity of deionized water in a china dish to obtain a homogeneous solution. The china dish was then introduced into a muffle furnace maintained at 500 ± 20°C. The solution ignites and burns with a flame, thereby yielding a voluminous solid mass. The dish was immediately removed from the furnace. Then the voluminous and foamy product was gently milled using a mortar and pestle. Afterwards, the product was directly used for characterization.

X-ray diffraction data were recorded on an X'Pert Pro Diffractometer (Panalytical) using CuK $\alpha$  radiation to ascertain the phase purity of the prepared samples. The energy dispersive X-ray (EDX) unit attached to the SEM was used to study the chemical composition of the prepared samples. Electron paramagnetic resonance (EPR) studies of the powdered samples were done on a JEOL FE1X ESR Spectrometer, operating in the X-band frequency with a field modulation of 100 kHz.

## 3. Results and discussion

Figure 1 shows the XRD pattern of the BAM:Mn sample obtained after the combustion process which



almost matched with the standard ICDD pattern number 26-0163 corresponding to BaAl<sub>10</sub>MgO<sub>17</sub> crystallized in a hexagonal lattice. The lattice parameters and some of the lattice planes responsible for major peaks (for the XRD pattern) are listed in Table-1. The EDX spectrum and the corresponding chemical mapping of the elements present in the BAM:Mn host is presented in figure 2 (a) and (b) which confirm the incorporation of Mn ions in to the BAM host.

Figure 3 (a) shows the EPR spectrum of BAM:Mn phosphor observed at 296 K. This spectrum shows the signal with the effective g value at  $g \approx 2.0$  due to Mn<sup>2+</sup> ions. The hyperfine structure centred at  $g \approx 2.0$  is due to Mn<sup>2+</sup> ions in tetrahedral symmetry [7]. The population of spin levels (N) can be calculated by comparing the area under the absorption curve with that of a standard (CuSO<sub>4</sub>·5H<sub>2</sub>O) of known concentration. Weil and Bolton [8] wrote the following formula including the experimental parameters of both the sample (x) and the standard (std):

$$\frac{N}{(A_x(\text{scan}_x)2G_{\text{std}}(B_m)_{\text{std}}(g_{\text{std}})2[S(S+1)]_{\text{std}}(N_{\text{std}}))} = \frac{(A_{\text{std}}(\text{scan}_{\text{std}})2G_x(B_m)_x(g_x)2[S(S+1)]_x)}{..(1)}$$

where A is the area under the absorption curve, scan is the magnetic field corresponding to the unit length of the chart, G is amplitude, B<sub>m</sub> is the modulation amplitude, g is the g factor, S is the spin of the ions in the ground state (S=5/2 for Mn<sup>2+</sup> ions and 1/2 for Cu<sup>2+</sup> ions). The subscripts 'x' and 'std' denote the sample and the standard respectively. N<sub>std</sub> denotes number of spins in 100 mg of CuSO<sub>4</sub>·5H<sub>2</sub>O standard. The number of spins increases with the decrease of temperature from 296 to 110 K. EPR spectra of BAM:Mn phosphor observed at 110 K is not shown. This is in accordance with the Boltzmann distribution law.

The Gibbs' energy can be determined using the expression [9, 10]

$$\Delta G = 2.303 RT \log_{10} (kBT) / (\lambda h) ..(2)$$

where ΔG is the Gibbs energy, R is the Universal gas constant (8.31 J/K/mol), kB is the Boltzmann constant (1.38 x 10<sup>-23</sup> J/K), T is the absolute temperature, λ is the reaction rate constant and is equal to the number of spins per m<sup>3</sup>, h is Planck's constant (6.63x10<sup>-34</sup> Js). The Gibbs energy of the Mn<sup>2+</sup> ions in BAM:Mn phosphor at  $g \approx 2.0$  has been computed to be -61.08 and -23.91 kJ/mol at 296 and 113 K, respectively. This calculated value is in good agreement with the value reported for glasses and minerals [11, 12]. The Gibbs free energy increases with the decrease of temperature. This value indicates the stability of this phosphor. Lower the value, higher the stability.

Thus the stability of this phosphor is high at 296 K. The negative sign indicates that there is strong attractive interaction between Mn<sup>2+</sup> ions and the phosphor matrix. The negative sign also indicates that the reaction between Mn<sup>2+</sup> ions is spontaneous and exothermic. In this process, the heat energy is given off in the reaction. The magnetic susceptibility can be determined using the following expression [13].

$$\chi = (N g^2 \beta^2 J (J+1)) / 3k_B T ..(3)$$

Here N is number of spins/m<sup>3</sup>,  $g \approx 2.0$ , β is Bohr magneton, J is total angular momentum quantum number, k<sub>B</sub> is Boltzmann constant and T is absolute temperature. The magnetic susceptibility of Mn<sup>2+</sup> ions in BAM:Mn phosphor at 296 K is found to be 91.85 x 10<sup>-3</sup> m<sup>3</sup>/kg. The magnetic susceptibility decreases from 296 to 110 K. The calculated magnetic susceptibility value is in good agreement with the value reported in the literature [11, 12]. The empirical Curie constant can be determined using the formula [14].

$$C = (N g^2 \beta^2 J (J+1)) / 3k_B ..(4)$$

The symbols have their usual meaning. The Curie constant at 296 K is found to be 27.18 emu/mol and its' value at 110 K is found to be 37.97 emu/mol. The Curie constant increases with the decrease of temperature. The measured Curie constant is consistent with the value reported in literature [12]. The Curie constant indicates the nature of paramagnetic interactions.

The experimental effective magnetic moment can be determined using the expression [15]

$$\mu_{\text{eff}} = (\sqrt{3k_B C}) / \sqrt{N} .. (5)$$

The theoretical magnetic moment value for a free Mn<sup>2+</sup> is 5.9 μB. The experimental value is found to be 5.9 μB at 296 and 110 K. The experimental magnetic moment value is equal to the theoretical magnetic moment value. This indicates that high spin Mn<sup>2+</sup> ions are present in the phosphor. The equality of theoretical and experimental magnetic moment indicates that the orbital angular momentum L is quenched. The value of the magnetic moment is indicative of the effective spin quantum number S. The zero-field splitting parameter D can be calculated from the ratio of



intensity of allowed hyperfine lines corresponding to the selection rule  $\Delta m = 0$  using the following expression [16].

$$I_m \propto 2 - (A^2(35 - 4m^2)) / (2(g\beta H)^2 -$$

$$(5.334D^2) / (g\beta H)^2 -$$

$$(35.14D^2(35 - 4m^2)) / (g\beta H)^2 + (208D^4(35 - 4m^2)^2) /$$

$$(g\beta H)^4 \dots$$

(6)

where  $m$  is the nuclear spin magnetic quantum number,  $I_m$  the intensity of the  $m_{th}$  allowed hyperfine (HF) line,  $A$  is the hyperfine splitting constant,  $D$  is the zero-field splitting parameter and the rest of the symbols have their usual meaning. The zero-field splitting (zfs)  $D$  arises due to a combined action of the spin-orbit (and electronic spin-spin) coupling taken as perturbation on the ligand field (LF) states [17]. The zfs parameter for this phosphor is found to be 32 and 33 mT at 296 K and 110 K, respectively. The hyperfine splitting constant (hfs)  $A$  can be calculated using the following expression [18].

$$B_m = B_0 - A_m - (35 - 4m^2) A^2 / 8B_0 \dots(7)$$

where  $B_m$  is the magnetic field corresponding to  $m \leftrightarrow m$  hyperfine line,  $B_0$  is the resonance magnetic field. The  $A$  value is thus found to be 8.46 mT at 296 and 110 K. The  $A$  value is independent of temperature variation. The strength of hfs depends on the matrix into which the ion is dissolved and is mainly determined by the electronegativity of the anion neighbours. This means that the magnitude of the hfs constant 'A' provides a qualitative measure of the ionicity of bonding between the  $Mn^{2+}$  ion and its ligands. van Wieringen [19] empirically determined a positive correlation between 'A' and the ionicity of the manganese-ligand bond. On this observation, it is found that the bonding between  $Mn^{2+}$  ions and the surroundings in this phosphor is ionic in character. In tetrahedral  $T_d$  or octahedral  $O_h$  symmetry,  $Mn^{2+}$  ion exhibits a sextet hyperfine structure centred at  $g \approx 2.0$  [20]. A value for  $O_h$  and  $T_d$  symmetry are 10 and 8.3 mT [20]. In the present case, we observed  $A$  value as 8.46 mT at 296 and 110 K. Therefore the site symmetry is tetrahedral since  $A$  value is nearer to 8.3 mT. The details of the 'g' values, number of spins ( $N$ ), Gibbs free energy ( $\Delta G$ ), magnetic susceptibility ( $\chi$ ), Curie constant ( $C$ ), effective magnetic moment ( $\mu_{eff}$ ), zero-field splitting parameter, and hyperfine splitting constant

(A) for  $Mn^{2+}$  ions in BAM:Mn phosphor at 296 and 110 K are given in Table 2.

#### 4. Conclusions

Sample of  $Mn^{2+}$ -doped  $BaMgAl_{10}O_{17}$  was synthesized by a solution combustion technique. The route for production of phosphors represents a fast, facile and inexpensive synthetic method. The hexagonal structure of the as-prepared  $Mn^{2+}$ -doped  $BaMgAl_{10}O_{17}$  phosphor was confirmed using the XRD technique. The EDX studies confirmed the incorporation of Mn ions in to the BAM host. Existence of 2+ manganese species in the phosphor was confirmed from the EPR data. From the temperature dependent EPR data it was observed that the number of spins increases with the decrease of temperature. In addition, Gibbs free energy, magnetic susceptibility, Curie constant, effective magnetic moment, zero-field splitting parameter, and hyperfine splitting constant (A) for the paramagnetic species was also evaluated from the data.

#### 5. Acknowledgements

This research was supported by Basic Science Research Program through the National Research Foundation of Korea (NRF) funded by the Ministry of Education (2017R1D1A1B03030003).

#### References

- [1] Y.-S.Cho, Y.-D. Huh, J. Alloys Compd. 737 (2018) 699
- [2] T.W. Kang, K.W. Park, G. Deressa, J.S. Kim, J. Lumin. 194 (2018) 551.
- [3] R. Cao, D. Peng, H. Xu, S. Jiang, Z. Luo, H. Ao, P. Liu, J. Lumin. 178 (2016) 388.
- [4] Y. Wang, J. Zhang, Y. Song, X. Yuan, J. China Univ. Geosci. 17 (2006) 272.
- [5] Z. Wu, Y. Dong, J. Jiang, J. Alloys Compd. 467 (2009) 605.



[6] P. Yang, G.-Q. Yao, J.-H. Lin, Opt. Mater. 26 (2004) 327.

[7] A. Abragam, B. Bleaney, Electron Paramagnetic Resonance of Transition Ions, Clarendon Press, Oxford, 1970.

[8] J.A.Weil and JR Bolton (2007) Electron Paramagnetic Resonance:Elementary Theory and Practical Applications. Wiley, New York.

[9] G. Sivaramaiah, Y. Pan, Phys. Chem.Miner.39 (2012) 515.

[10] Wigner, Eyring, Polanyi, and Evans, Trans. State Theory Chem. React. (1930).

[11] G. Sivaramaiah, J.L. Rao,Spectrochim. Acta Part A98 (2012) 105.

[12] G. Sivaramaiah, J. Lin, Y. Pan, Phys. Chem. Miner. 38 (2011) 159.

[13] A.J. Dekker, Solid State Physics, Department of Electrical Engineering, University of Groningen, Netherlands (2006).

[14] C. Kittel, Introduction to Solid State Physics, seventh edition, John Wiley & Sons, Inc., NewYork (1996).

[15] A.M. Hashem, H.M. Abuzeid, D. Mikhailova, H. Ehrenberg, A. Mauger, C.M.Julien, J. Mater. Sci. 47 (2012) 2479.

[16] B.T. Allen, J. Chem. Phys. 43 (1965) 3820.

[17] C. Rudowicz, S.K.Misra, Appl. Spectrosc. Rev. 36 (1) (2001) 11.

[18] R. Aasa, J. Chem. Phys 52 (1970) 3919.

[19] J.S.van Wieringen, Discuss. Faraday Soc. 19 (1955) 118.

[20] R.W.A Franco, J.F.Lima, C.J.Magon, J.P.Donoso, Y.Messaddeq, J. Non-Cryst Solids 352 (2006) 3414.

Table 1: XRD data of BAM:Mn, ( $\lambda= 0.15406$  nm)

2 $\theta$ values	Intensity	d value	h k l	Lattice parameters
15.64	25	5.66	0	Hexagonal Lattice
18.6	35	4.76	1	
19.75	65	4.49	1	

21.65	17	4.1	1	with a= 5.62 c= 22.65
23.58	35	3.77	0	
24.03	25	3.70	1	
26.83	25	3.32	1	
31.59	40	2.83	0	
32.78	17	2.73	1	
35.21	100	2.695	1	
35.60	55	2.52	1	
39.73	35	2.26	0	
42.09	35	2.13	2	
44.14	40	2.05	1	
57.63	25	1.59	2	
58.68	20	1.57	2	
58.9	17	1.56	1	
66.5	25	1.40	2	

**Table 2:** Various EPR parameters for the BAM:Mn system; g value, number of spins (N), Gibbs free energy ( $\Delta G$ ), magnetic susceptibility ( $\chi$ ), Curie constant (C), effective magnetic moment ( $\mu_{eff}$ ), zero-filed splitting parameter (D) and hyperfine splitting constant (A).

T	'g	N	$\Delta G$	$\chi$	C	$\mu$	D	'A'
(K)	(u)	(Spi ns/m <sup>3</sup> )	(kJ /m <sup>3</sup> ol)	(m <sup>3</sup> /k g)	(em u/m ol)	$\mu_{eff}$	(m T)	valu e
29	2.	37.3	-	91.	27.1	5.	3	
6	0	9	61.	85	8	9	2	8.46
		$\times 10^2$	08	x		1		
				$10^{-3}$				
11	2.	52.2	-	34.	37.9	5.	3	
0	0	2 x	23.	51	7	9	3	8
		$10^{22}$	91	x		1		.
				$10^{-3}$				4
								6

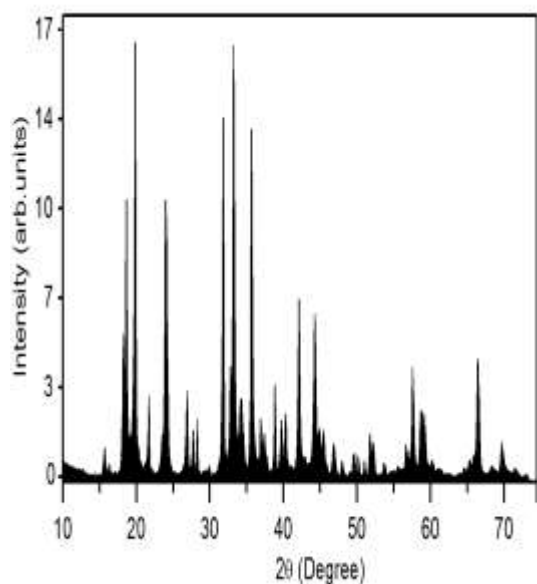


Figure 1: XRD pattern of BAM:Mn phosphor

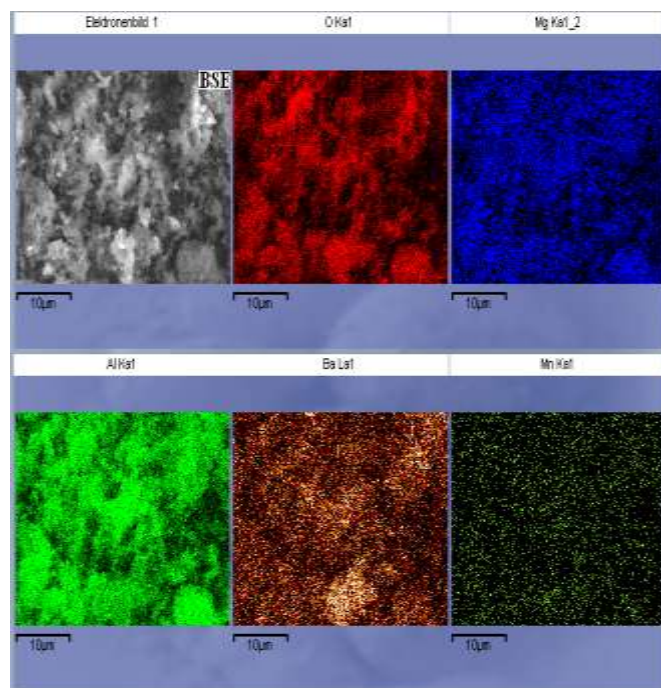


Figure 2(b): Chemical mapping of BAM:Mn phosphor

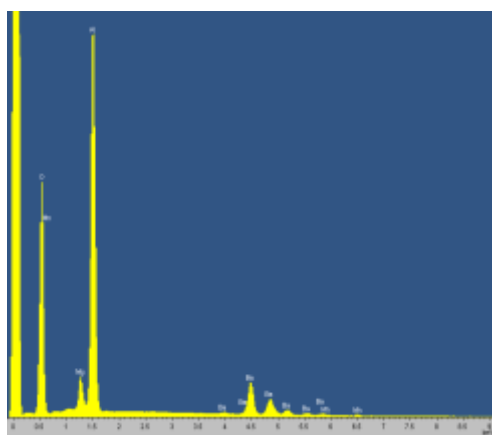


Figure 2(a): EDX spectrum of BAM:Mn phosphor

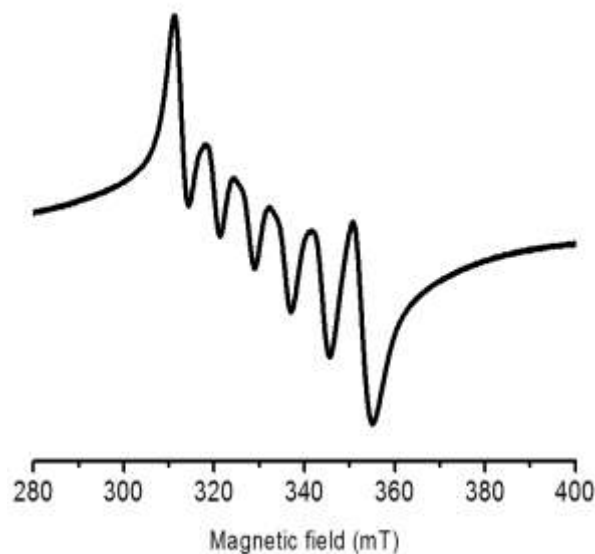


Figure 3: EPR spectrum of BAM:Mn phosphor at room temperature

### References

- [1] Ahmed M Choudhary, MA Khan (1988) Technological Studies on Citrus & Ginger Fruit based drink Nucleus 23(314): 41-45.



[2] Gatchalian, MM & S.Y.Deleon (1992) Introduction to Food Tech Manila, Philippines Merriam & Book store, Inc 130-131.

[3] Sikder, SS (1999), Production of ready to eat drink mango juice & Studies of Storage Life.

[4] Altman R.D. Marcussen K.C (2001). Effect of a ginger extract on knee pain in patient with osteoarthritis Rheum, 44(11), 2531-2538.

[5] Bordia A, Verma SK, Srivastava K.C effect of Ginger & Fenugreek on blood lipid, blood sugar & platelet aggregation in patient with Coronary artery disease Prostaglandis Leukot Egg Fatty Acids 1997: 56(5): 379-384.

[6] Ranganna S.2011 Handbook of analysis of quality control for fruit and vegetable products 2nd Edition, Tata Mc Graw Hill Pub. Co. Ltd, New Delhi.

[7] Babasaheb B.D.2000. Handbook of nutrition and diet, Processing and preservation of mixed chips from potato, papaya and carrot.

[8] Langner (1998) Ginger history & use. Advances in Therapy 25(1), 25-44.

[9] Benavenle Garcia & J. Castillo J Agric Food chem. 2008, Update on uses and properties of Citrus Flavonoids : New Findings in Anti cancer & Cardiovascular & anti inflametory activity. 56(15) pp. 6185-6205.

[10] Shahnah SM, S. Ali, H..Ansari & P.Bagri 2007 New Sequiterpene Denivitae from fruit peel of citrus lemon (Limn) Burrl F.Sci, Pharma, 75: 165-170.

[11] Jenny Joseph & Sangeeta Shukla 2015 Preparation & quality evaluation of mixed fruit squash Int. Jr. of Advance Industrial Engg. Vol.3 No.3. Quality assessment of mixed fruit squash, physico chemical analysis and sensory evaluation and storage study.

[12] J.S.Jothi, P. Karmoker and K. Sarower (2014) Quality assessment of mixed fruit squash, physico chemical analysis and sensory evaluation and storage study J.Bangladesh Agri 12(1) : 195-201.